

# Sparse Bayesian ARX models with flexible noise distributions

Johan Dahlin, Adrian Wills and Brett Ninness\*

December 1, 2021

## Abstract

This paper considers the problem of estimating linear dynamic system models when the observations are corrupted by random disturbances with nonstandard distributions. The paper is particularly motivated by applications where sensor imperfections involve significant contribution of outliers or *wrap-around* issues resulting in multi-modal distributions such as commonly encountered in robotics applications. As will be illustrated, these nonstandard measurement errors can dramatically compromise the effectiveness of standard estimation methods, while a computational Bayesian approach developed here is demonstrated to be equally effective as standard methods in standard measurement noise scenarios, but dramatically more effective in nonstandard measurement noise distribution scenarios.

**Keywords:** Bayesian inference, Hamiltonian Monte Carlo, Gaussian mixture models.

arXiv:1801.01242v1 [stat.ME] 4 Jan 2018

---

\*E-mail addresses to authors: `firstname.lastname@newcastle.edu.au`. JD and AW are with the School of Engineering, The University of Newcastle, Australia. BN is with the Faculty of Engineering and Built Environment, The University of Newcastle, Australia. This work was supported by the Australian Research Council Discovery Project DP140104350.

# 1 Introduction

Robust identification of dynamical systems is an important problem in many practical applications. Outliers and other un-modelled mechanisms naturally occur in many real world situations, and failure to consider and adapt to them can have seriously detrimental effects on the quality of system estimates. In this paper, we consider and illustrate the potentially dramatic effect of noise distribution mis-modelling and develop a solution that can adapt to a very wide range of noise distributions without detriment to system parameter estimates.

In particular, we consider a novel Bayesian approach to dynamic system estimation which we illustrate using the very commonly employed auto-regressive exogenous input (ARX) model structure:

$$A(q)y_t = B(q)u_t + e_t, \quad (1)$$

where  $y_t \in \mathbb{R}$  and  $u_t \in \mathbb{R}$  denotes the output and input of the system at time  $t$  respectively and the system polynomials are given by

$$A(q) = 1 + \sum_{k=1}^{n_a} a_k q^{-k}, \quad B(q) = \sum_{k=1}^{n_b} b_k q^{-k} \quad (2)$$

where  $a_{1:n_a} \triangleq \{a_k\}_{k=1}^{n_a}$  and  $b_{1:n_b}$  denote the unknown system polynomial coefficients. Here, it is assumed that the system orders  $n_a$  and  $n_b$  are unknown parameters to be estimated from data.

To be able to handle a wide range of noise distributions, we assume that the noise  $e_t$  can be modelled using a Gaussian mixture model (GMM),

$$p(e_t) = \sum_{k=1}^{n_e} w_k \mathcal{N}(e_t; \mu_k, \sigma_k^2), \quad \sum_{k=1}^{n_e} w_k = 1, \quad (3)$$

where  $w_k$ ,  $\mu_k$  and  $\sigma_k$  denote the weight, mean and standard deviation of the mixture component  $k$ , respectively. The GMM can successfully capture the behaviour of many types of non-standard (eg. non unimodal Gaussian) but commonly encountered distributions including multi-modal, skewed and heavy tailed cases.

The main contributions of this paper are:

- (i) the introduction of a novel Bayesian approach for ARX model estimation, hereafter referred to as BARX and;
- (ii) proposing an efficient sampling scheme for Bayesian inference in this model.

The main features of the BARX estimated model is that:

- (a) it includes sparsity promoting priors to automatically determine the required model orders  $n_a$  and

$n_b$  from data and;

- (b) the inclusion of a GMM to model the noise. The GMM also includes sparsity promoting priors to determine the flexibility required from the input-output data set provided to the inference algorithm.

The inference is carried out using Hamiltonian Monte Carlo (Neal, 2010, Betancourt, 2017), which will be referred to by the abbreviation HMC and is an efficient Markov chain Monte Carlo (MCMC) scheme for estimating high dimensional posterior distributions.

We offer three numerical illustrations of our Bayesian BARX approach using synthetic and real-world data. These establish that the approach can perform well in different scenarios and that its data-driven nature is able to correctly estimate ARX model parameters, model orders and noise distributions.

Related work in System Identification includes Dahlin et al. [2012] and Troughton and Godsill [1998], which also consider Bayesian methods for estimating the orders of ARX models. However, the main difference in this work is the use of a GMM for the noise distribution, which can cover many interesting special cases.

Mixture models for regression problems like the ARX model are also popular in Statistics, where e.g., Malsiner-Walli et al. [2016] consider similar problems but makes use of Gibbs sampling and do not consider time series models, only regression. Baldacchino et al. [2017] considers a mixture of Student's  $t$  distributions for a class of time series models (not ARX). They use variational Bayes to estimate the posterior.

## 2 Sparse Bayesian modelling

This paper employs a Bayesian approach to the estimation of the model orders, system parameters and noise mixture model coefficients in the model structure (1)-(3). Delivering this rests on two key aspects - the selection of priors on all components to be estimated and provision of a means to combine these with the data likelihood to provide posterior estimates. In this section we will address prior distribution selection.

### 2.1 System polynomial coefficients

The estimation of the system polynomials is basically a linear regression problem. In the Bayesian setting, this requires us to choose a prior distribution for the coefficients. The typical choice is a uniform distribution or a Gaussian distribution, which leads to a closed-form expression for the posterior if the likelihood is Gaussian. These priors are known as conjugate priors in the Bayesian literature, see e.g., Bishop [2006] or Murphy [2012] for more information. Furthermore, the use of a Gaussian prior is equivalent to  $L_2$ -regularised least squares.

In this work, we assume a different prior that induces sparsity - unnecessary coefficients in an over-parametrized model are shrunk towards zero. This allows us to select a maximum model order for the system polynomials and the sparsity promoting mechanism will decide the appropriate model order from the data.

The optimal sparsity promoting prior should have a large probability mass at zero and long tails to accommodate for possible large system polynomial coefficients. A prior with these qualities is the following one:

$$[a_{1:n_a} b_{1:n_b}] \sim \mathcal{N}(0, \sigma_f^2), \quad \sigma_f \sim \mathcal{C}_+(0, 1), \quad (4)$$

where  $\mathcal{C}_+(\mu, \gamma)$  denotes the Cauchy distribution restricted to be positive with location  $\mu \in \mathbb{R}$  and scale  $\sigma > 0$ .

This choice corresponds to a so-called horseshoe prior, which exhibits the above desired properties since the Cauchy distribution puts a large fraction of its probability mass around its mode while also possessing infinite variance. However, it has tails that decay geometrically and therefore coefficients will be shrunk towards zero if there is no evidence in the data saying otherwise.

The horseshoe prior has been shown to perform better (in the MSE sense) in regression problems than e.g., a Laplacian or Gaussian priors, see e.g., Polson and Scott [2010] and Armagan et al. [2011]. These benchmarks and promising results in a pilot study (not presented here) are the main reasons for this choice of prior distribution.

## 2.2 Noise distribution

The noise distribution is given by the GMM in (3) with unknown order, weights, means and variances. This is a powerful and versatile model class that covers many different interesting distributions as illustrated in Figure 1.

Here, the green histograms present the data simulated from four different distributions (orange lines): a uniform distribution, a GMM, a skewed Gaussian and a heavy-tailed Student's  $t$ . Light green histograms overlain on these orange lines are derived from sample realisations of GMM's seeking to represent these distributions with the solid green line being a kernel density estimates formed from these histograms. The GMM distribution components are shown in shaded grey with their summation as a solid grey line.

Note that in all these cases the GMM can successfully model all of these distributions using only five components. As a consequence, the model structure (1)-(3) will be able to accommodate all these types of noise distributions without prejudicing the quality of the estimates of the system polynomials  $A(q)$ ,  $B(q)$ .

A popular approach for Bayesian inference in mixture models is to assume a non-parametric prior

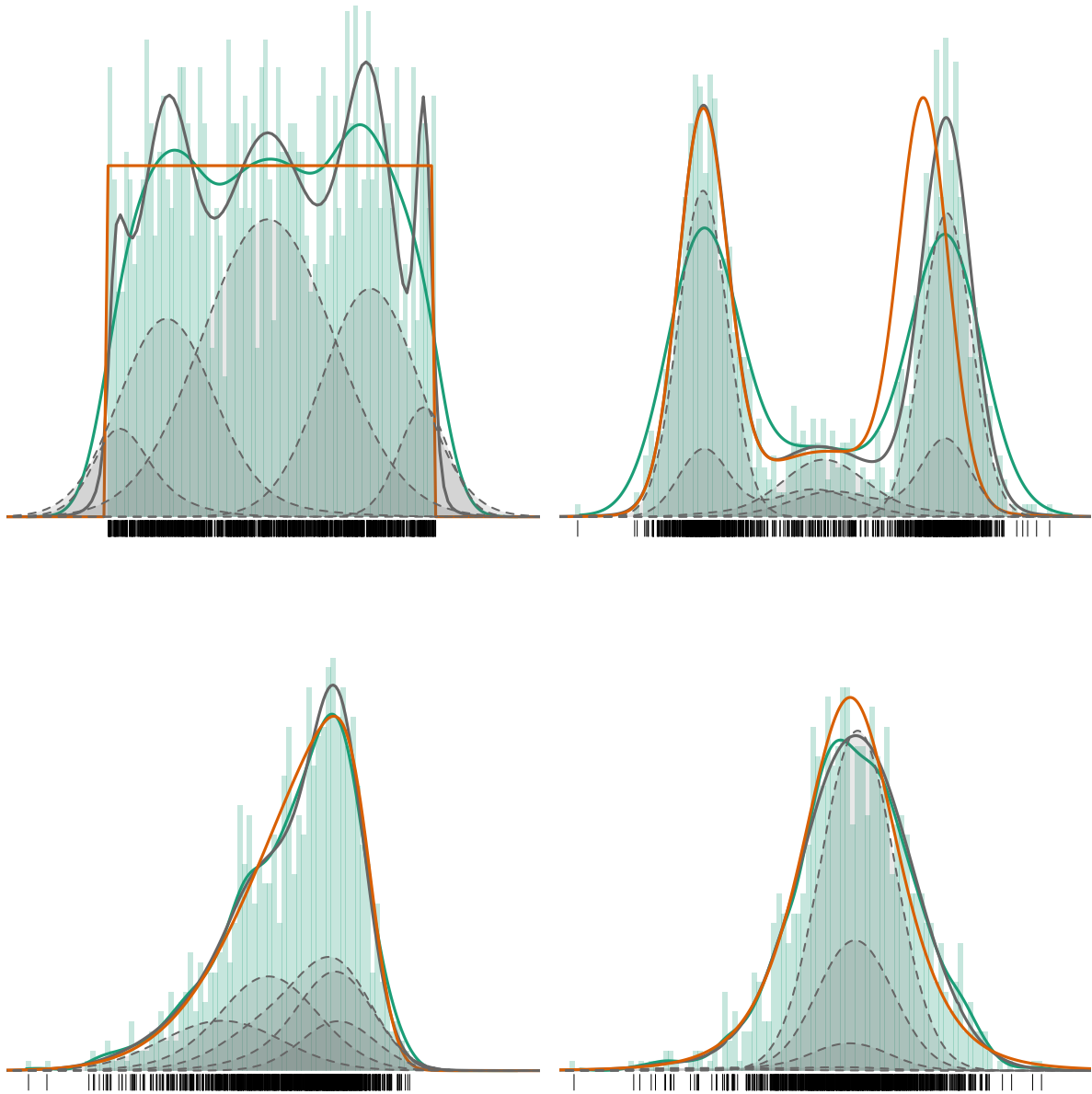


Figure 1: Four examples of GMMs for capturing the behaviour of the noise: uniform noise (top left), multi-modal noise (top right), skewed noise (bottom left) and heavy-tailed noise (bottom right). The histogram of the generated data is presented together with the kernel density estimate (green lines) and the GMM approximation (orange lines). The mixture components in the GMM are presented as gray lines and areas.

known as the Dirichlet process (DP; Gelman et al., 2013) on the mixture weights. The benefit of a DP is that it automatically determines the number of components required to describe the data and is flexible in the sense that this number increases with the number of observations.

However the drawback is that inference in such models can be challenging, especially using common MCMC methods such as the Metropolis–Hastings (MH) method as realisations from the associated Markov chain can exhibit poor mixing which results in a large computational burden. Furthermore, the fact that the expected number of components grows with the amount of data is not desirable in our setting as the aim is to find the correct number of components of the noise distribution.

Instead, we make use of recent progress in introducing sparsity in over-parameterised Bayesian finite mixture models. This allows for more efficient inference and avoids the numerical challenges connected with infinite mixture models. To achieve this, as in (4) we assume a sparsity inducing prior for the component means

$$\mu_{1:n_e} \sim \mathcal{N}(0, \sigma_\mu^2), \quad \sigma_\mu \sim \mathcal{C}_+(0, 1),$$

Moreover, we follow the recommendations by Gelman et al. [2013] and also select a half-Cauchy distribution as the prior for  $\sigma_{1:n_e}$ ,

$$\sigma_{1:n_e} \sim \mathcal{C}_+(0, 5),$$

which corresponds to a weakly informative prior on  $\sigma_{1:n_e}$ .

Finally, we assume a Dirichlet prior (DP) for the mixture weights

$$w_{1:n_e} \sim \mathcal{D}(e_0, \dots, e_0),$$

where  $n_e$  denotes the maximum number of components that could be present in the mixture. The Dirichlet distribution is a standard choice in Bayesian mixture models as it is a distribution over the simplex, which means that the sum of  $w_{1:n_e}$  is one at all times. Furthermore, it is also the appropriate conjugate prior for the multinomial distribution, which allows for closed-form expressions for the posterior of the mixture weights.

The Dirichlet distribution can be used to introduce sparsity in the mixture by setting  $e_0$  to a small number. This results in only a few weights receiving the majority of the probability mass and therefore creating a mixture with a few active components if the data does not strongly support more active components.

A popular choice introduced by Ishwaran and Zarepour [2002] is to select  $e_0 = 0.1n_e^{-1}$  as the value of the hyperprior. This empties superfluous components of the mixture and mimics the behaviour of the

DP with concentration parameter 0.1 asymptotically [Rousseau and Mengersen, 2011].

However, empirical studies by e.g., Miller and Harrison [2013] have suggested that DP's typically over-estimate the number of components. Another option is to use a hyper-prior for the concentration parameter as proposed by Malsiner-Walli et al. [2016],

$$e_0 \sim \mathcal{G}(\alpha_w, n_e \alpha_w), \tag{5}$$

which is a Gamma distribution with mean  $n_e^{-1}$  and variance  $(\alpha_w n_e^2)^{-1}$ . Hence a large value of  $\alpha_w$  results in a prior that is concentrated around  $n_e^{-1}$  with a small variance. If  $n_e$  is large, this results in that only a few components are a priori given a large mixture weight. This intuition is validated empirically by Malsiner-Walli et al. [2016] which argue that this approach with  $\alpha_w = 10$  usually recovers a mixture with the correct number of components. We have also seen evidence supporting this in our preliminary work (not presented here). Note that the consistency results obtained by Rousseau and Mengersen [2011] also holds in this case and this is the reason for choice of (5) as the prior structure for the mixture weights in this paper.

### 3 Hamiltonian Monte Carlo Computation of Posteriors

The parameter vector for the BARX model is given by

$$\theta = \{a_{1:n_a}, b_{1:n_b}, w_{1:n_e}, \mu_{1:n_e}, \sigma_{1:n_e}, \sigma_\mu, e_0\}, \tag{6}$$

which needs to be estimated from the input-output data. Having specified the priors for these parameters, we now turn to the question of how to combine these priors with the likelihood of the observed data to deliver the required Bayesian posterior estimates.

We approach this via a computational Bayesian approach wherein a Markov chain is constructed with an invariant density which it will converge to being equal to the desired Bayesian posterior of interest. That is, we construct a random number generator that generates realisations from the Bayesian posterior and use sample means and histograms from this random number generator as approximate Bayesian estimates.

This is a standard so-called MCMC approach, and the common MH method in this class operates by taking realisations from any *proposal* Markov chain with transition probability  $\gamma$ :

$$\theta_{k+1} \sim \gamma(\theta_{k+1} | \theta_k) \tag{7}$$

and then modulating this arbitrary Markov chain by only accepting those proposals with probability  $\alpha$

given by

$$\alpha(\theta_{k+1} | \theta_k) = \frac{\pi(\theta_{k+1})}{\pi(\theta_k)} \cdot \frac{\gamma(\theta_k | \theta_{k+1})}{\gamma(\theta_{k+1} | \theta_k)} \quad (8)$$

where  $\pi(\cdot)$  is the *target distribution* which in our case is

$$\pi(\theta) = p(\theta | y_{1:T}). \quad (9)$$

This is a very simple algorithm, but unfortunately its effectiveness is very much dependent on how well the proposal density  $\gamma(\cdot)$  is *tuned* to the target density  $\pi(\cdot)$ . If the two are not similar then the acceptance probability  $\alpha$  either rejects a great majority of proposals  $\theta_{k+1}$  that propose any significant movement, or accepts a high proportion of tiny movements, and in both cases generates highly correlated realisations with very poor sample average convergence rates to underlying true estimates.

HMC [Neal, 2010, Betancourt, 2017] methods address this problem by replacing the target density  $\pi(\theta)$  in the acceptance probability computation (8) by one over a higher dimensional space  $\exp(-H(\theta, p))$  which involves an additional auxiliary scalar *momentum* variable  $p$  (which is eventually ignored) and Hamiltonian in position  $\theta$  and momentum  $p$  given by

$$H(\theta, p) = -\log \pi(\theta) + \frac{1}{2} p^\top M^{-1} p, \quad (10)$$

where  $M$  is a user define *mass matrix*. The acceptance probability is then modified to

$$\alpha(\theta_{k+1} | \theta_k) = \exp(-H(\theta_{k+1}, p_{k+1}) + H(\theta_k, p_k)). \quad (11)$$

The proposals  $\theta_{k+1}, p_{k+1}$  are generated by randomly moving the auxiliary momentum variable according to

$$p_{k+1} \sim \mathcal{N}(0, M^{-1}),$$

and then generating  $\theta_{k+1}$  by simulating the energy preserving Hamiltonian dynamics

$$\frac{\partial \theta_i}{\partial t} = \frac{\partial H(\theta, p)}{\partial p_i}, \quad \frac{\partial p_i}{\partial t} = -\frac{\partial H(\theta, p)}{\partial \theta_i} \quad (12)$$

over a user chosen time period. The intuition is that at the proposal stage, the random movement of momentum to  $p_k$  kicks a hockey puck on a frictionless ice surface to a new position proposal  $\theta_{k+1}, p_{k+1}$  of equal combined potential and kinetic energy.

Since the gradient of the Hamiltonian with respect to  $\theta$  is the same as the gradient of the log-posterior then simulating the dynamics (12) helps guide the Markov chain towards areas with high



posterior probability, possibly via quite large moves thereby decreasing autocorrelation of realisations.

Not only is the proposal  $\theta_{k+1}$  then adapted to the target  $\pi(\theta)$ , but furthermore, due to energy invariance of the Hamiltonian dynamics (12) the marginal invariant distribution of the realisations  $\{\theta_k\}$  are left unchanged at  $\pi(\theta)$  once the auxiliary  $p_k$  momentum realisations are discarded.

## 4 Numerical illustrations

We provide three different numerical illustrations to investigate the properties and the performance of the proposed BARX model using both synthetic and real-world data.

In each of the illustrations, the *same* model structure and algorithmic settings are used and the *only* difference is the input-output data supplied to the algorithm. All implementation details are summarised in Appendix A and the source code with data is available via GitHub, see Section 5 for more information.

### 4.1 Synthetic data with Gaussian noise

We generate a data set with  $T = 1,000$  observations using the system polynomial coefficients

$$a_{1:2} = \{-1.5, 0.7\}, \quad b_{1:3} = \{0, 1, 0.5\},$$

using a pseudo-binary input signal and adding standard Gaussian noise to the output signal.

The BARX estimate model is compared with the results of the ARX command in MATLAB combined with a cross-validation scheme to find the model order. Regarding the latter, we partition the estimation data into two sets of equal length and make use of the first part for estimating models where  $n_a$  and  $n_b$  varies between 1 and 5. The model order is selected as the one that minimises the squared prediction error computed on the second part. This approach selects  $n_a = 3$  and  $n_b = 5$ .

Figure 2 summarises the results obtained from the experiment. In the top plot, the validation data set (dots) is presented together with the one-step-ahead predictors obtained via the BARX model (orange) and MATLAB (purple). We note that the predictors are virtually the same for most time steps. Using the predictors, the model fit is computed on validation data by

$$\text{MF} = 100 \left( 1 - \frac{\sum_{t=1}^{T_v} (y_t - \hat{y}_t)^2}{\sum_{t=1}^{T_v} (y_t - \bar{y})^2} \right),$$

where  $\hat{y}_t$  and  $\bar{y}$  denote the one-step-ahead predictor and the sample mean of the output signal, respectively. We obtain the model fit 96.6% and 96.5% for ARX and BARX, respectively. This indicates that the BARX model can replicate the result of the ARX command in MATLAB for models with unimodal Gaussian noise and thereby offers a good sanity check of BARX.

The middle and bottom plots in Figure 2 present the estimates of the system polynomial coefficients

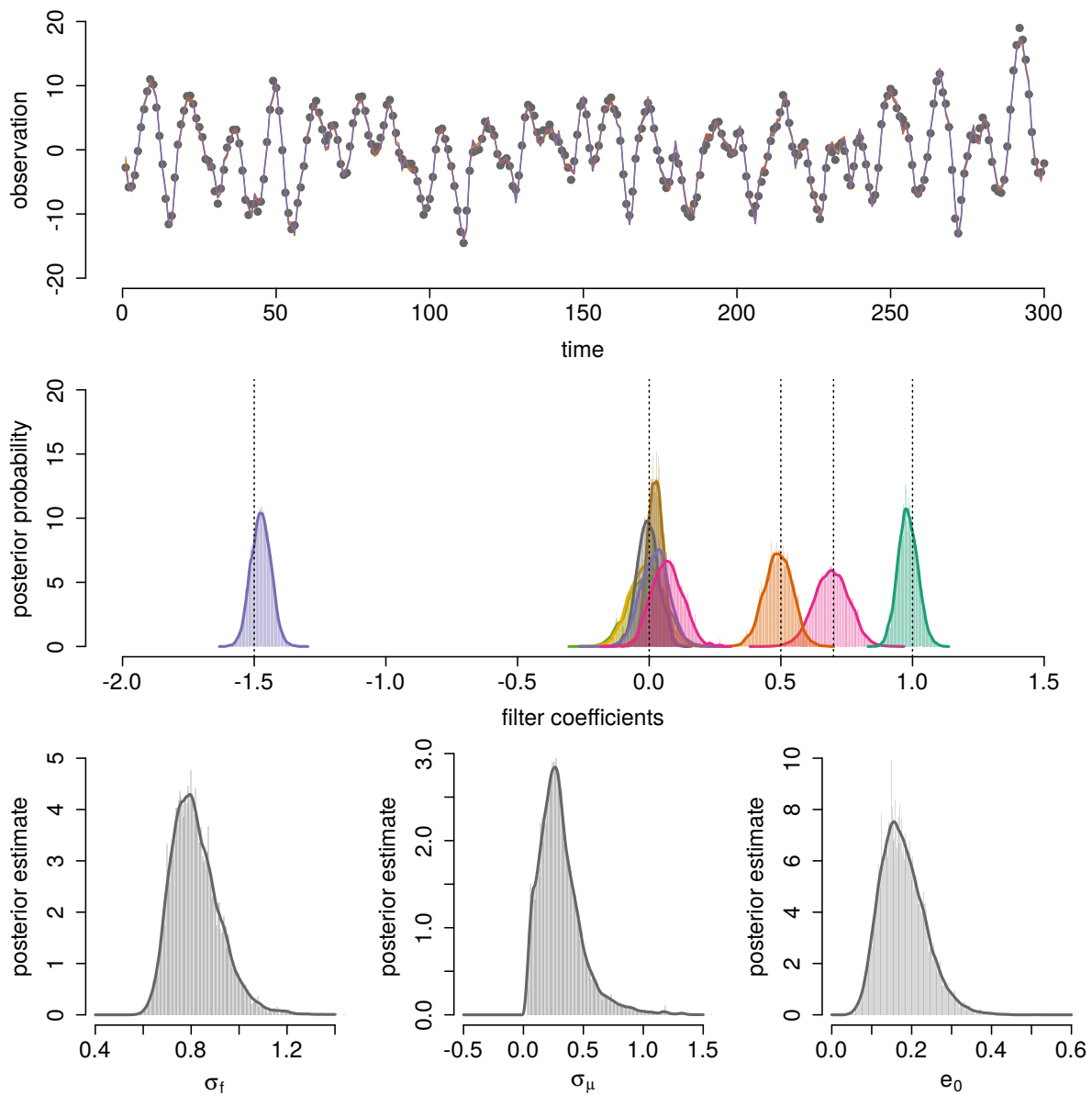


Figure 2: Top: the one-step-ahead predictors for the ARX (purple) and BARX (orange) models versus validation data (dots) in the ARX model with Gaussian noise. The estimated posteriors of the system polynomial coefficients (middle) and priors (bottom) are also presented. Dotted vertical lines indicate the true system coefficients.

and the estimates of the prior distributions for the BARX model, respectively. Note that the sparsity of the horseshoe prior in the system polynomial coefficients has shrunk most of system coefficient posteriors towards zero. At least four coefficients do not overlap zero and therefore remain statistically significant, which corresponds well to the model from which the data was generated.

From the posteriors of the priors, we can see that the prior for the system polynomial coefficients can accommodate larger deviations from zero than the prior for the mixture means. This is reasonable as some of the system polynomial coefficients are quite far from zero. Finally, we note that the prior on the mixture weights indicates a sparse behaviour as it is quite small and therefore promotes a few mixture components to have large weights with the rest being small.

## 4.2 Synthetic data with Gaussian mixture noise

We continue with a more interesting example where the output is corrupted with noise from a GMM that generates a significant sequence of *outliers* as might occur in practice due to sensor imperfections.

We generate a data set with  $T = 1000$  observations from an ARX system (1) with system polynomials (2) having coefficients:

$$a_{2:3} = \{-0.25, 0.2\}, \quad b_{1:3} = \{0, 1, 0.5\},$$

and being driven by an exogenous input  $u_t$  being an i.i.d. zero mean and unit variance Gaussian process. The observations  $y_t$  involve a corruption sequence  $e_t$  which are i.i.d. realisations from a GMM (3) given by:

$$p(e_t) = 0.4 \cdot \mathcal{N}(e_t : 7, 1) + 0.6 \cdot \mathcal{N}(e_t : 0, 1).$$

This means that the mean of the noise switches between 0 and 7 due to some unknown underlying process. The model fit for this data set obtained by the ARX command in MATLAB using the same model order estimation as in Section 4.1 is  $-0.22\%$ .

This poor performance is due to the obvious violation of the Gaussian noise assumption, but it can be challenging to validate these assumptions in practice. To compare, we fit the BARX model to the same data to see how its data-driven properties handle the bi-modal noise distribution.

Figure 3 presents the results from the run of the BARX model. In the top part, in orange we see the high posterior density (HPD) intervals of the posterior of the one-step-ahead predictor obtained from BARX together with the same predictor (in purple) from ARX and the validation data (dots). Note that the predictor from ARX tries to capture the bi-modality by adjusting the mean but this has the negative consequence that the predictor is performing poorly as no data is found in the gap between the two modes.

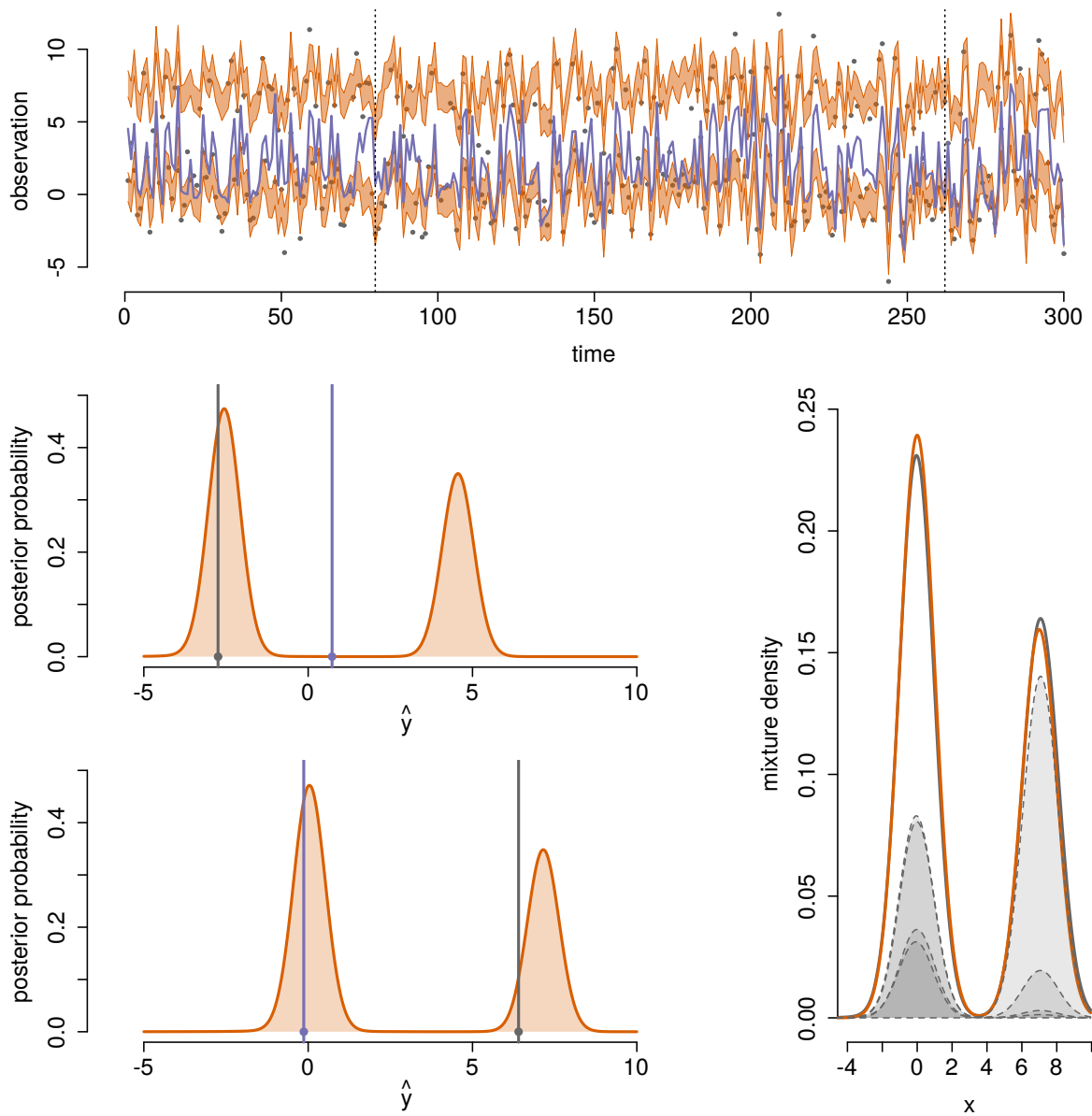


Figure 3: BARX with noise from a Gaussian mixture. Top: validation data with predictions from ARX (purple) and BARX (orange). Bottom: posterior estimates of the noise distribution (left) and the components of the GMM modelling the noise (right).

In the lower left part of the figure, we present two slices of the top plot at times indicated by the vertical dotted lines on the top plot. The posterior of the predictor (orange) covers the observation (gray vertical line) at both time points. However, the ARX predictor (purple vertical line) is quite far off from the observation in both cases, which is the explanation for the bad model fit. In the lower right, we present the true noise distribution (orange) together with the BARX estimate (gray) and its constituting components (gray shaded areas).

The BARX predictor is bi-modal as the noise distribution is bi-modal and this information could be beneficial for e.g., stochastic MPC. It also highlights the benefit of working with distributions of quantities instead of point-estimates, which are the standard approach in likelihood-based System Identification methods.

### 4.3 Real-world EEG data

Finally, we revisit a real-world EEG data set analysed in Dahlin et al. [2012], where the authors assume an ARX model with Student's  $t$ -distributed noise. We apply the same procedure as before to estimate the BARX model. Note that this data set does not contain any input signal, so that that  $B(q) = 0$  is known in this example.

Figure 4 presents the results of the BARX estimated model. The one-step-ahead predictors seem to perform well and this is reflected in a high model fit of 92.3% on validation data for the BARX model, which is a substantial increase from the model fit of 85.6% obtained in Dahlin et al. [2012]. Moreover, we note that the estimated noise of the data set is clearly not Gaussian, as the behaviour of the tails is very different. An interesting finding from this experiment is that only  $\{a_1, a_2, a_4, a_5, a_6, a_7\}$  seems to be non-zero and contribute to the predictor.

## 5 Conclusions

The numerical illustrations indicate that the results of the proposed BARX estimated model approach developed in this paper can be useful in problems where non-standard measurement noise corruptions cause traditional system estimation approaches to fail by a significant margin.

At the same time, the BARX approach was illustrated to perform equivalently to standard approaches where the measurement noise assumptions underlying standard approaches apply. As a result the BARX estimation approach developed here can be considered a *robust* method in that its default application safeguards failure in non-standard situations without sacrificing performance in standard settings.

For the user, no special calibration is required for the BARX method proposed here and in that sense it is an automated method or data-driven model that adapts its complexity to capture the dynamic behaviour observed in the input-output dataset.

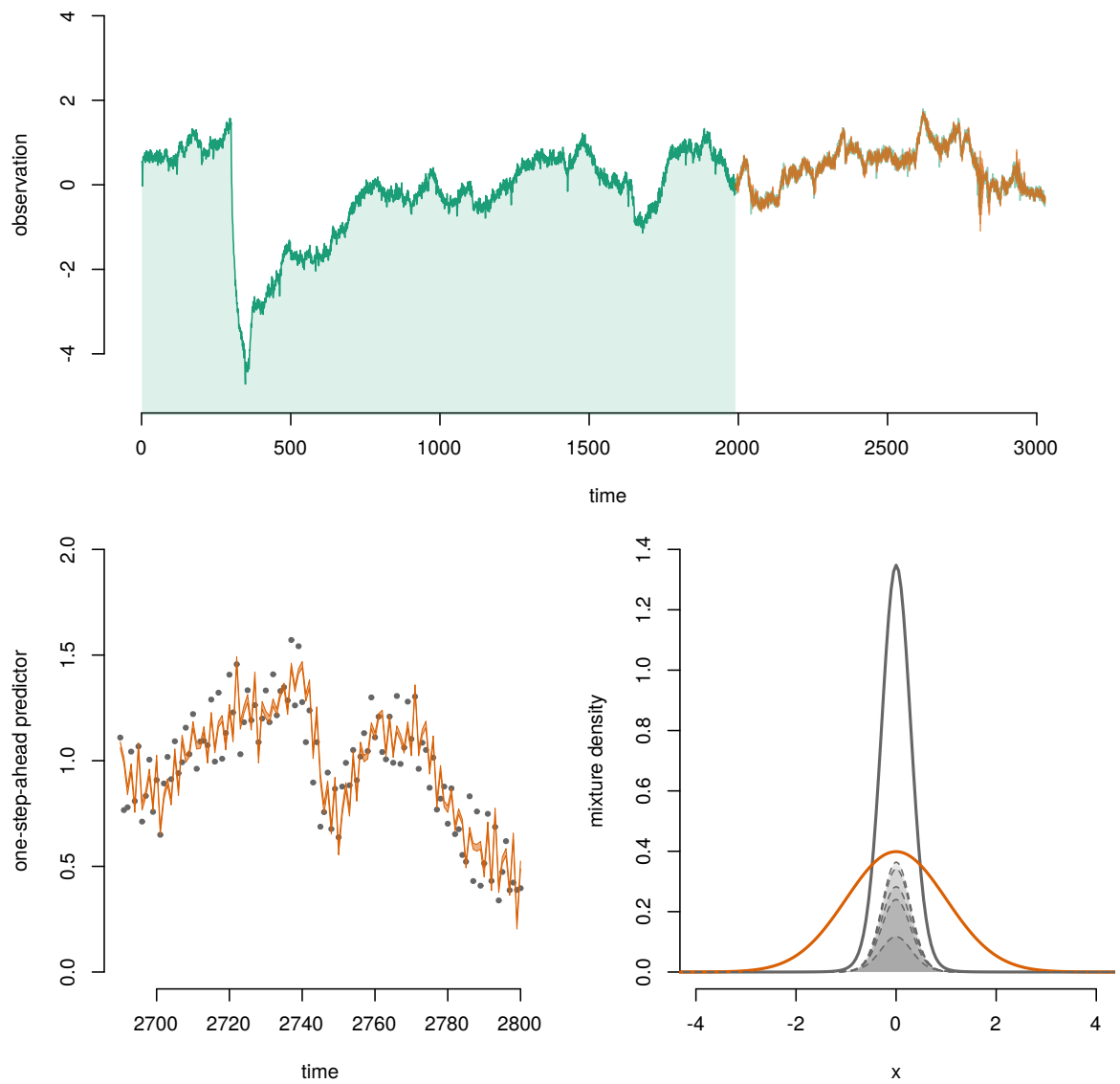


Figure 4: BARX model estimated on real-world EEG data. Top: the estimation data (shaded green) and validation data set (unshaded green) are presented together with the one-step-ahead predictor (orange). Bottom left: zoom-in of top plot with validation data indicated by dots. Bottom right: the estimate of the noise distribution with the best Gaussian approximation (orange) to the estimation data.

Future work includes the generalisation of the work here to model structures more flexible than ARX such as Box-Jenkins transfer function models. It would also be interesting to integrate this inference approach with MPC to create controllers that can handle e.g., multi-modal or heavy-tailed noise.

The source code and data used in this paper as well as some supplementary material are available from GitHub <https://github.com/compops/barx-sysid2018/> and via Docker (see `README.md` in the GitHub repo). The code is written mainly in Python and is distributed under an open-source license.

## A Implementation details

The implementation details are almost the same for all three illustrations in Section 4. In the first two experiments, we make use of a maximum order of 5 for the system polynomials, i.e.,  $n_a = n_b = 5$  and use  $n_e = 5$  components for the noise distribution mixture. In the third experiment, we set  $n_a = 10$  and  $n_b = 0$  (as no input data is available). These values have not been calibrated in any way and were just selected arbitrarily. The hyperpriors are selected as described in Section 2.

The HMC sampler is implemented using the STAN software [Stan Development Team, 2017], which makes use of NUTS [Hoffman and Gelman, 2014] to decide on the number of steps and their lengths. We run the sampler for 30,000 iterations and discard the first 15,000 iterations as burn-in.

The initialisation of the system coefficients and the means of the mixture components greatly influences the accuracy of the estimates. We therefore initialise the former randomly over the interval  $(-1, 1)$  and the latter on an equally spaced grid over the range of the output data. All mixture weights are initialised as  $1/n_e$  and the remaining parameters are initialised as 1.

## References

- A. Armagan, M. Clyde, and D. B. Dunson. Generalized beta mixtures of Gaussians. In *Proceedings of the 2011 Conference on Neural Information Processing Systems (NIPS)*, Granada, SP, December 2011.
- T. Baldacchino, K. Worden, and J. Rowson. Robust nonlinear system identification: Bayesian mixture of experts using the t-distribution. *Mechanical Systems and Signal Processing*, 85:977–992, 2017.
- M. Betancourt. A conceptual introduction to Hamiltonian Monte Carlo. *Pre-print*, 2017. arXiv:1701.02434.
- C. M. Bishop. *Pattern recognition and machine learning*. Springer Verlag, New York, USA, 2006.
- J. Dahlin, F. Lindsten, T. B. Schön, and A. Wills. Hierarchical Bayesian ARX models for robust

- inference. In *Proceedings of the 16th IFAC Symposium on System Identification (SYSID)*, Brussels, Belgium, July 2012.
- A. Gelman, J. B. Carlin, H. S. Stern, D. B. Dunson, A. Vehtari, and D. B. Rubin. *Bayesian data analysis*. Chapman & Hall/CRC, 3 edition, 2013.
- M. D. Hoffman and A. Gelman. The No-U-turn sampler: Adaptively setting path lengths in Hamiltonian Monte Carlo. *Journal of Machine Learning Research*, 15(1):1593–1623, 2014.
- H. Ishwaran and M. Zarepour. Dirichlet prior sieves in finite normal mixtures. *Statistica Sinica*, 12(3): 941–963, 2002.
- G. Malsiner-Walli, S. Frühwirth-Schnatter, and B. Grün. Model-based clustering based on sparse finite Gaussian mixtures. *Statistics and computing*, 26(1-2):303–324, 2016.
- J. W. Miller and M. T. Harrison. A simple example of Dirichlet process mixture inconsistency for the number of components. In *Proceedings of the 2013 Conference on Neural Information Processing Systems (NIPS)*, Lake Tahoe, USA, December 2013.
- K. P. Murphy. *Machine learning: a probabilistic perspective*. The MIT Press, 2012.
- R. M. Neal. MCMC using Hamiltonian dynamics. In S. Brooks, A. Gelman, G. Jones, and X-L. Meng, editors, *Handbook of Markov Chain Monte Carlo*. Chapman & Hall/CRC Press, 2010.
- N. G. Polson and J. G. Scott. Shrink globally, act locally: Sparse Bayesian regularization and prediction. *Bayesian Statistics*, 9:501–538, 2010.
- J. Rousseau and K. Mengersen. Asymptotic behaviour of the posterior distribution in overfitted mixture models. *Journal of the Royal Statistical Society: Series B (Statistical Methodology)*, 73(5):689–710, 2011.
- Stan Development Team. Stan: A C++ library for probability and sampling, version 2.14.0, 2017. URL <http://mc-stan.org/>.
- P. T. Troughton and S. J. Godsill. A reversible jump sampler for autoregressive time series. In *Proceedings of the 23rd International Conference on Acoustics, Speech, and Signal Processing (ICASSP)*, Seattle, USA, May 1998.